Spin and charge excitations in optimally doped $Bi_2Sr_2CaCu_2O_{8-\delta}$

M. Rübhausen
Institut für Angewandte Physik und Zentrum für Mikrostrukturforschung, Universität Hamburg, Jungiusstraße 11, 20355 Hamburg, Germany

P. Guptasarma and D. G. Hinks
Materials Science Division and Science and Technology Center for Superconductivity, Argonne National Laboratory, 9700 S. Cass Avenue, Argonne, Illinois 61801

M. V. Klein
Department of Physics and Science and Technology Center for Superconductivity, Universitiy of Illinois, 104 S. Goodwin Avenue, Urbana, Illinois 60439

(Received 6 January 1998)

We present Raman spectra of low- and high-energy charge and spin excitations in $Bi_2Sr_2CaCu_2O_{8-\delta}$ single crystals with an optimized critical temperature of 95 K. The prominent feature of the high-energy background at around 250 meV is a rearrangement of spectral weight in B_{1g} and $A_{1g}+B_{2g}$ symmetry below the critical temperature, similar to the observations in underdoped and optimally doped $Y_{1-x}Pr_xBa_2Cu_3O_{7-\delta}$ compounds. The B_{1g} spectra can be attributed to magnetic scattering and exhibit below the critical temperature an increase of scattering intensity indicating an enhanced magnetic coherence in the superconducting state. Scattering in A_{1g} geometry reflects more incoherent electronic contributions. There, we observe a decrease of scattering intensity for energies around 120 meV similar to the observations made in superconductor-insulator-superconductor tunneling spectroscopy or at half that energy with superconductor-insulator-normal tunneling spectroscopy and angle-resolved photoemission spectroscopy. The resonance enhancement of the rearrangement is rather strong with a maximum above 2.71 eV laser-excitation energy. In the low-energy region, which is influenced by the effects at higher energies, a gap feature in B_{1g} symmetry is observed yielding a value for the magnitude of the superconducting order parameter of $\Delta = 34$ meV. This gap feature is influenced by the orthorhombicity of the crystals and except for a small loss of spectral weight below 25 meV, no gap feature is visible in A_{1g} scattering geometry. Our experimental results raise questions about the applicability of the conventional theories for the electronic Raman scattering of the cuprate superconductors, which neglect the interplay between low- and high-energy excitations. [S0163-1829(98)05929-3]

I. INTRODUCTION

High-temperature superconductors (HTSC) reveal many unexpected properties when compared to traditional superconductors that can be understood within the framework of the BCS theory. Clearly, two of the most important features are a predominantly $d_{x^2-y^2}$ order parameter[1–3,34] and the existence of strong antiferromagnetic short-range order in the cuprate superconductors. Another important aspect concerns changes in the excitation spectrum at rather high energies below the critical temperature (T_c) observed by superconductor-insulator-normal (SIN) conductor and superconductor-insulator-superconductor (SIS) tunneling spectroscopy,[4] angle-resolved photoemission spectroscopy (ARPES),[2,5] and Raman spectroscopy.[6] These changes reveal that the energy scale that describes the effects of superconductivity is not uniquely set by the value of the superconducting order parameter Δ but also by J, the value of the superexchange energy.

Raman spectroscopy is one of the experimental techniques providing information about low- and high-energy excitations of the HTSC.[7–14] It has clarified the importance of antiferromagnetic and charge excitations in this class of materials. The Raman spectra from the antiferromagnetic precursor phases of the HTSC are dominated by a broad antiferromagnetic two-magnon excitation[15–20] and sharp phonon structures at excitation energies below 0.1 eV.[21–23] Whereas the observed spectral features and their line shapes in the antiferromagnetic regime are understood to some extent,[19,24] the description of the high-energy response in doped and superconducting materials still causes severe problems.[25] Upon doping holes into the precursors, the high-energy excitation broadens and shifts towards lower energies, but it persists in the metallic phase even for optimally doped samples.[7,13,26]

It is well established that in optimally doped compounds a signature of the superconducting gap for energies of the order of 2Δ can be seen in the Raman response.[3,12] The interpretation of the experimental data relies on theories that are based on the approach of Klein and Dierker[27] using the mass part of the interaction of light with superconducting electrons of a conventional electron gas exhibiting a gap in its excitation spectrum. Deveraux *et al.*[3] have argued that the different energies for the pair-breaking peak in A_{1g}, B_{1g} and B_{2g} symmetry seen in the superconducting state of the HTSC not only indicate an anisotropic order parameter, but different frequency dependencies can be expected in the limit of small Raman shifts for d- and s-wave order parameters. In particu-

lar, for a d-wave order parameter one would expect an ω^3 power law for B_{1g} symmetry. However, experimentally it is found for $Bi_2Sr_2CaCu_2O_{8-\delta}$ that an approximate ω^3 power law applies for Raman shifts up to energies of 2Δ.[3] Though some progress has been made in fitting the observed line shapes and reproducing the observed relative scattering intensities for different polarization geometries,[28] these model calculations invoke neither interactions between low- and high-energy excitations, i.e., the incoherent part of the electronic response, nor any resonance Raman effects. The importance of resonance effects for the gap feature has been already demonstrated by Kang *et al.*,[29] who found for $Tl_2Ba_2CuO_6$ that the intensity and the power law depends on the laser-excitation energy.

Recently, Rübhausen *et al.* found in underdoped and optimally doped Y-123 compounds a superconductivity-induced effect at high energies of the order of 250 meV, i.e., roughly at 8Δ.[30,6] The observed feature is very broad and for optimal doping it also influences the low-energy region. Thus, this effect reveals a subtle aspect of the interaction between the low- and high-energy excitations.

Here, we present Raman spectra that illuminate the relevance of changes induced by superconductivity in the high-energy excitations and discuss their importance for understanding of the low-energy features in the context of charge and spin excitations. Moreover, we show that superconductivity-induced effects at high energies are most likely a general property of the HTSC as they occur in both BSCCO-2212 and Y-123 families of the cuprate superconductors. We also try to make connections to the results obtained by other experimental techniques, such as ARPES, SIS, and SIN spectroscopy.

II. EXPERIMENT

We studied single crystals of $Bi_2Sr_2CaCu_2O_{8-\delta}$ (BSCCO-2212) that were grown using a variation of the travelling solvent floating zone process in a double-mirror IR image furnace (NEC SC-M15HD) modified with an external homebuilt control for very slow growth. Growth was carried out without solvent from high density, carbonate-free, single phase rods. Absence of impurities, nearly perfect stoichiometry, and high cationic homogeneity yielded sharp superconducting transitions at 95 K. The transition shown in Fig. 1 at 95 K has a width of less than 1 K and is the highest transition temperature yet obtained from the pure BSCCO-2212 phase.

Raman spectra were recorded with a Dilor XY multichannel set up equipped with a liquid-nitrogen-cooled backilluminated charge coupled device and corrected for the spectral response as described elsewhere.[18] During the measurements, which were perfomed on freshly cleaved surfaces, the samples were placed in a closed-cycle cryostat and measured over the temperature range from 10 to 300 K. We focused the light from an Ar-ion laser with excitation wavelengths of 458, 476, 488, 502, and 514 nm to a spot of 100 μm diameter using power densities of 10 to 50 W/cm^2. This resulted in an effective temperature-dependent heating[31] of between 5 and 20 K calculated using the known thermal conductivity of BSCCO.[32] In presenting the spectra, we give values for the effective temperatures. All spectra have been corrected for the thermal-Bose factor. In order to denote the scattering geometries, we use the Porto notation as described elsewhere in detail.[6] The two important scattering geometries denoted as $z(x,y)\bar{z}$ and $z(x,x)\bar{z}$ correspond for BSCCO essentially to B_{1g} and $A_{1g}+B_{2g}$ when assuming a tetragonal lattice. In the figures, we use Raman shifts in units of cm^{-1}, which are roughly converted to meV when divided by eight.

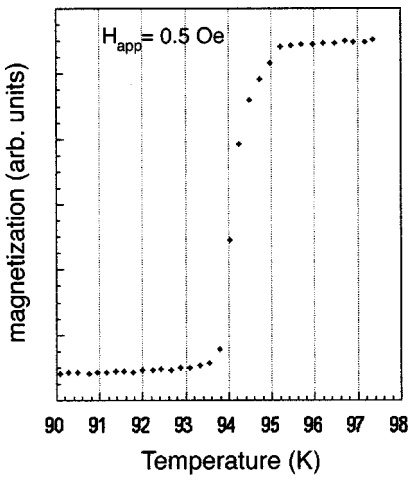

FIG. 1. Magnetically measured transition temperature of an optimally doped BSCCO-2212 single crystal. T_c is 95 K, the transition width is below 1 K.

III. RESULTS AND DISCUSSION

In Fig. 2 we present the low-energy Raman data from a BSCCO-2212 single crystal using an excitation energy of 2.41 eV in $z(xx)\bar{z}$ and $z(xy)\bar{z}$ scattering geometry at temperatures of 14 and 100 K. The spectra show the well-known symmetry dependencies of the phonon modes.[22,23] In B_{1g}

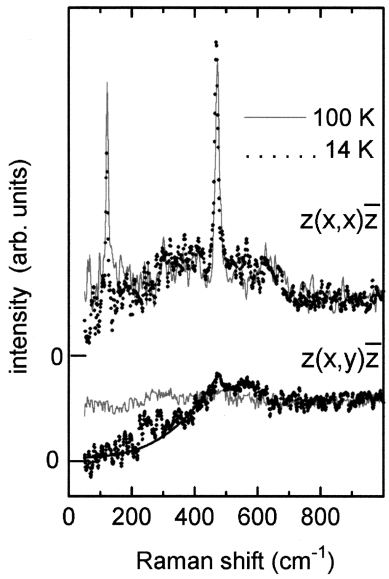

FIG. 2. Raman spectra taken from 50 to 1000 cm^{-1} in $A_{1g}+B_{2g}$ and B_{1g} symmetry as denoted in Porto notation at 100 K (solid line) and 14 K (dots). The spectra reveal the well-known symmetry-dependent phonons and the opening of a gap in B_{1g} geometry. The bold solid line is a ω^3 fit to the data. The spectra are shifted upwards as indicated.

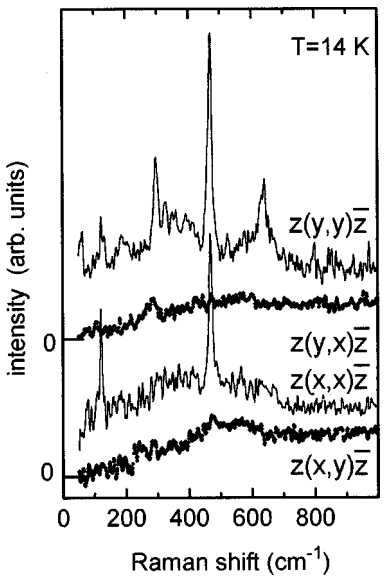

FIG. 3. Raman data from 50 to 1000 cm^{-1} in $A_{1g}+B_{2g}$ and B_{1g} symmetry as denoted in Porto notation at 14 K. The spectra reveal the well-known influence of the orthorhombicity on the phonons. The spectra are shifted upwards as indicated.

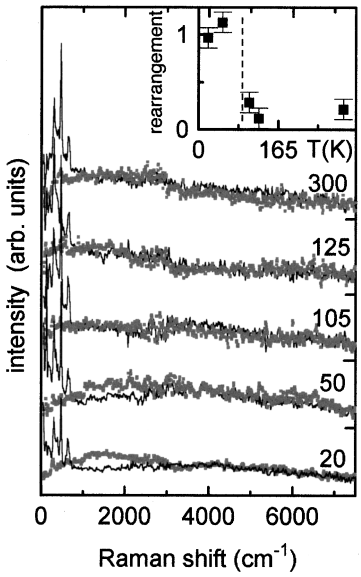

FIG. 4. Raman data from 50 to 7500 cm^{-1} for various temperatures. The $A_{1g}+B_{2g}$ (solid line) and B_{1g} (dotted line) responses are scaled to match above 3000 cm^{-1}. The spectra are shifted upwards and temperatures are given in the figure. The inset shows the integrated difference for the different scattering symmetries, i.e., the temperature dependence of the rearrangement.

symmetry, hardly any phonon feature can be observed. Therefore, this scattering geometry probes predominantly the charge and spin responses and enables us to identify unambiguously the pair-breaking peak and the corresponding power laws below T_c. The gap feature is clearly visible and appears around 500 cm^{-1}, leading to a maximum value of $2\Delta/k_BT_C \approx 7$. The power law exhibits a nonlinear behavior and is to a good approximation proportional to ω^3 as indicated by the bold solid line. The absence of any clear gap feature in $A_{1g}+B_{2g}$ symmetry is remarkable, as a peak at slightly lower energies than for B_{1g} symmetry has previously been observed for single crystals with a T_c of $\approx$90 K.[33] Instead, we observe a small decrease of spectral weight below 200 cm^{-1}. This reduction of spectral weight might indicate an opening of a gap in this scattering geometry at much smaller frequencies than for B_{1g} symmetry and, in turn, would indicate a much larger anisotropy of the order parameter than usually observed in other Raman experiments.[33]

The influence of the orthorhombicity on the Raman spectra is shown in Fig. 3. The dependence of the phonon modes on the x and y directions of the crystal axis has been previously observed by Liu *et al.*[22] The modes at 129, 180, 295, and 630 cm^{-1} are especially strong in $z(yy)\bar{z}$ geometry. In $z(yx)\bar{z}$ geometry the phonon at 285 cm^{-1} is analogous to the strong B_{1g} feature in $YBa_2Cu_3O_7$.[23] Moreover, the B_{1g} spectra reveal the influence of the orthorhombicity on the gap feature. The pair-breaking peak around 500 cm^{-1} is more prononounced in $z(xy)\bar{z}$ than in $z(yx)\bar{z}$ geometry. Furthermore, the scattering intensities in the low-energy limit are different for the two polarization geometries. In $z(xy)\bar{z}$ geometry the intensity fluctuates around zero below 150 cm^{-1} and exhibits more clearly a ω^3 power law than the scattering intensity in $z(yx)\bar{z}$ geometry, which is more linear and whose scattering intensity is above zero for the lowest measured frequency of 45 cm^{-1}. An influence of the orthorhombicity on the gap feature is not surpising, given that the mass part of the interaction of light with electrons in the solid can be easily related to the band structure,[27] which in turn becomes influenced by the orthorhombicity.

Even more important is the influence of the Raman continuum, which exceeds energies of more than 1 eV, on the pair-breaking peak. Figure 4 shows the high-energy continuum between 6 meV and 1 eV for $A_{1g}+B_{2g}$ (solid line) and B_{1g} (dots) geometry. In order to show the effect more clearly, we have scaled the $A_{1g}+B_{2g}$ data with a common factor of 0.70 ± 0.05. At 300 K a constant and featureless background is visible, and both scattering geometries match each other across the whole frequency range. This is very similar to the observations in underdoped and optimally doped Y-123 compounds.[7,9,13,14,30] Upon cooling no drastic changes are visible. Below T_c, changes of spectral weight occur in an energy range between 800 and 3000 cm^{-1} that are different in $A_{1g}+B_{2g}$ and B_{1g} symmetry. This is, again, analogous to the rearrangement in underdoped and optimally doped Y-123 compounds. It is worthwhile to remark that the traditional theories for the pair-breaking excitation neglect any effects of the high-energy background on the low-energy region. However, from our measurments it is clear that there is some interference between these two energy regions.

In the previous work of Rübhausen *et al.*[6] on the Y-123 compounds, we have carried out an analysis of the experimental data within the t-J model assuming an interaction Hamiltonian that consists of a superexchange (spin) and an effective-mass (charge) scattering term. The response function $R(\omega)$ can then be written as $R(\omega)=R^{\text{spin}}(\omega)+R^{\text{charge}}(\omega)+R^{\text{spin-charge}}(\omega)$. Here, $R^{\text{spin}}(\omega)$ is the response function of the superexchange mechanism alone leading to a damped two-magnon feature and $R^{\text{charge}}(\omega)$ is the response function from the incoherent density of states of an unconventional Fermi liquid.[36] The interference term $R^{\text{spin-charge}}(\omega)$ is due to mixed excitations of spins and

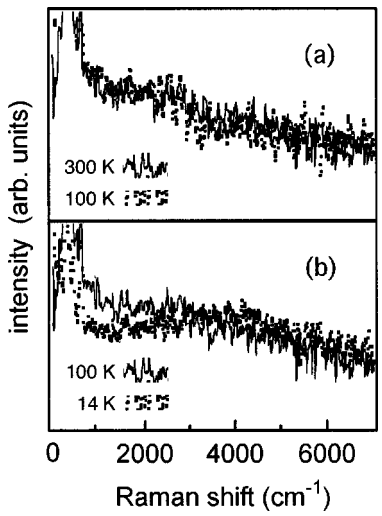

FIG. 5. Raman data from 50 to 7500 cm^{-1} for various temperatures. The $A_{1g}+B_{2g}$ reponses are shown at 300 K (solid) and 105 K (dots) in (a) and 300 K (solid) and 14 K (dots) in (b). The suppression of spectral weight is strongest around 1000 cm^{-1} in (b).

charges. For underdoped compounds we have found an enhanced scattering intensity in an energy range between 100 to 300 meV for temperatures of 200 to 100 K, most likely due to $R^{\text{spin-charge}}(\omega)$, which was not observed for optimally or overdoped samples. We have argued that this channel is characteristic of the system near an antiferromagnetic instability and might be related to the pseudogap regime.[6] As expected, in the optimally doped BSCCO, this contribution is clearly not apparent. Below T_c, the spin and charge system become less coupled due to the termination of scattering channels. Then the spectrum would be a simple superposition of charge and spin contributions. Hence, we interpret the broad peak around 1800 cm^{-1} in B_{1g} geometry as a damped two-magnon excitation. This view is supported by studies of Blumberg *et al.*,[26] who found in the BSCCO-2212 system a shift of the two-magnon peak towards lower energies which is consistent with the observation of the doping dependence of the two-magnon excitation in Y-123.[7,9,13,14]

In the following we carry out our analysis by investigating the observed symmetries separately. In Fig. 5(a) we display the $A_{1g}+B_{2g}$ symmetry for temperatures of 300 and 105 K. Clearly, as mentioned before, no change is visible above T_c. However, below T_c, Fig. 5(b) reveals a suppression of spectral weight starting below 1000 cm^{-1}. There is a small enhancement of spectral weight around 4000 cm^{-1} and above 6000 cm^{-1} no change of the scattering intensity is visible. When considering the A_{1g} response as strongly related to the incoherent electronic properties of the cuprates, it is quite tempting to relate our results to those obtained by ARPES, SIN, and SIS tunneling spectroscopy.[4,2,5] On these cases a suppression of the spectral weight related to the incoherent electronic states is also visible. Let us consider first the situation as encountered by Raman spectroscopy. There, we couple the light to a polarizability bubble and the observed scattering intensity can be expressed as $I(\omega) \propto \mathrm{Im}\,[R(\omega)]$ where

$$R(\omega)=\sum_{\mathbf{k},\mathbf{k}',\omega'} G_{\mathbf{k}'}(\omega+\omega')G_{\mathbf{k}}(\omega+)\Gamma_{\mathbf{k},\mathbf{k}'}(\omega,\omega'). \quad (1)$$

Here $\Gamma_{\mathbf{k},\mathbf{k}'}(\omega,\omega')$ is the vertex part that describes the coupling of light to the polarizability bubble, which is expressed by the particle propagators $G_{\mathbf{k}'}(\omega+\omega')$ and $G_{\mathbf{k}}(\omega')$. For the particle propagators, Dyson's equation applies, and for the vertex part, the Bethe-Salpeter equation applies. The Bethe-Salpeter equation consists of a term representing the bare vertex and a term that describes the interaction between two propagators. A change of the response function can be due to the propagators or the vertex part in Eq. (1). Of course, different experimental techniques have different bare vertices and the importance of vertex corrections can vary with the experimental probe. In a situation where strong contributions of incoherent scattering need to be considered, it is crucial not to neglect vertex corrections for, e.g., a Raman experiment. Vice versa, for SIS tunneling spectroscopy one can safely use the bare vertex, since the two propagators of Eq. (1) belong to different parts of the material and the interaction between them is small. Then the SIS tunneling experiment essentially displays the joint density of states of an electronic response, just as an electronic Raman spectrum, if one would be able to neglect vertex corrections. Therefore, it is very useful to compare both techniques in order to figure out the contribution of the vertex part for the Raman spectra. In SIS experiments a clear suppression of spectral weight having a minimum around 120 meV can be seen,[4] comparing well with the energy scale observed in the Raman experiments, where the strongest suppression occurs around 125 meV, i.e., 1000 cm^{-1}. However, the width of the feature in the SIS experiment is 90 meV or only a third of the width observed in the Raman spectra. The latter is most likely related to the vertex part, since additional vertex corrections would have the tendency to smear out the suppression. For a SIN experiment one of the propagators of Eq. (1) corresponds to a normal metal and its imaginary part is, in first approximation, constant. Hence, we are dealing with a summation over the imaginary part of the propagator representing the excitation in the superconductor. Therefore, the experiment shows the density of states related to the superconductor. The suppression of spectral weight as observed in Raman or SIS tunneling spectroscopy should be present as well, but on a lower energy scale. However, this energy scale should be comparable to the one observed by ARPES. Here, the measurements display the spectral function $A(\mathbf{k},\omega)\propto \mathrm{Im}[G(\mathbf{k},\omega)]$ for selected momenta in the Brillouin zone. Indeed, both experimental techniques show a suppression of spectral weight on energy scales that are very similar.[4,5] This qualitative agreement between the different experimental probes shows that the observed effects are driven by the propagators of Eq. (1) and not predominantly the vertex, even though the latter plays potentially an important role for the line-shape discription in the Raman spectra. In the Raman experiment the decrease of scattering intensity in A_{1g} geometry is accompanied by the enhancement of the B_{1g} scattering intensity. However, as discussed in the following, the latter scattering geometry corresponds to excitations having a magnetic rather than an electronic origin.

The effect of the superconducting transition on the magnetic excitations can be studied via the B_{1g} geometry as

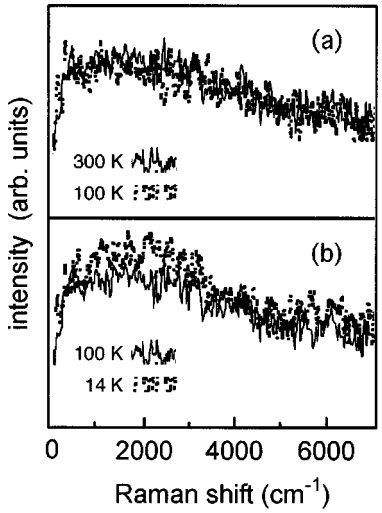

FIG. 6. Raman data from 50 to 7500 cm^{-1} for various temperatures. The B_{1g} reponses are shown at 300 K (solid) and 105 K (dots) in (a) and 300 K (solid) and 14 K (dots) in (b), respectively. An enhancement of the magnetic scattering around 2000 cm^{-1} is clearly visible.

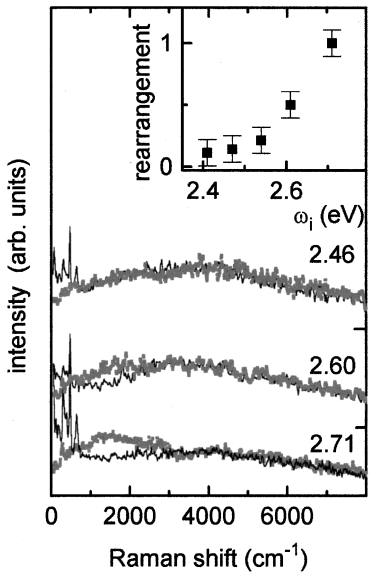

FIG. 7. Raman data from 50 to 8000 cm^{-1} for various excitation energies. The $A_{1g}+B_{2g}$ (solid line) and B_{1g} (dotted line) responses are scaled to match above 3000 cm^{-1}. The spectra are shifted upwards as indicated. The effective temperature is 20 K. The inset shows the resonance enhancement of the rearrangement towards a 3 eV laser-excitation energy.

shown in Fig. 6. The assignment that magnetic excitations are predominantly seen in B_{1g} geometry is based on investigations carried out in the antiferromagnetic regime and investigations regarding the doping dependence of the observed magnetic peaks.[8,6,14] In the antiferromagnetic precursor this selection rule is a direct consequence of the commutation relation of the Heisenberg model of antiferromagnetism and the Fleury-Loudon superexchange scattering Hamiltonian. Figure 6(a) shows results in B_{1g} geometries taken at 300 and 105 K. The spectra reveal a flat featureless background decreasing with frequency. No change with temperature is visible above T_c. Below T_c in Fig. 6(b), a clear enhancement of scattering intensity is visible in the frequency range between 600 and 3000 cm^{-1}. This enhancement of scattering intensity shows an enhanced coherence of the magnetic excitations, i.e., they are less damped. Combining this with the reduced scattering intensity in A_{1g} geometry, we conclude that it is most likely that a reduction of the scattering intensity of the incoherent electronic background occurs. This follows because the magnetic and electronic systems seem to become less coupled. Therefore the scattering intensity resulting from the coherent electronic and magnetic systems is enhanced. The enhanced coherence of the magnetic system is expressed by an increased scattering intensity of the magnetic peak and the enhanced coherence of the electronic system is expressed by, e.g., the existence of a pair-breaking peak around 500 cm^{-1}. Simple sum rules do not apply, since the Raman vertices coupling to coherent and incoherent states should be different.

It is well known, that the two-magnon excitation becomes resonant towards a 3 eV laser-excitation energy.[17,18,24,35,37,38] This has been interpreted in terms of a triple-resonance mechanism.[24,37,38] Therefore, an important aspect is the resonance enhancement of the rearrangement, as shown in Fig. 7. The enhancement of the rearrangement towards a 3 eV excitation energy is clearly visible in the data. In particular, the feature at 1800 cm^{-1} in B_{1g} becomes enhanced as well. This is qualitatively in good agreement with the study in slightly underdoped Y-123 materials showing a similar resonance enhancement.[30] However, for optimally doped BSCCO-2212 the increase of scattering intensity is much sharper and stronger than for the Y-123 system. The details of the resonance enhancement depend on the band structure of a given system. From Fermi-surface measurements it is known that the band structures of the BSCCO-2212 and the Y-123 systems are indeed different.[39] Thus, different details of the resonance enhancements are expected. This may give valuable hints about the intermediate electronic states involved in the scattering process as soon as a more detailed theory is available. Since the triple-resonance theory[24,37,38] has been rather successful in describing the resonance enhancement in the antiferromagnetic compounds, and since the resonance behavior is not radically changed in the doped systems, this theory might be a good start to improve nonresonant theories.

IV. CONCLUSION

We have investigated the low- and high-energy spin and charge responses of $Bi_2Sr_2CaCu_2O_{8-\delta}$ single crystals with an optimized T_c of 95 K by Raman spectroscopy, varying the temperature and the laser-excitation energy in order to clarify the influence of the superconducting transition on these excitations.

The low-energy data reveal a gap feature in B_{1g} symmetry around $2\Delta = 500$ cm^{-1} exhibiting a ω^3 power law for the intensity of the Raman shift below the gap frequency. This gap feature is influenced by the orthorhombicity of the crystals, and except for a small loss of spectral weight below 200 cm^{-1}, no indication of an opening of a gap can be seen in $A_{1g}+B_{2g}$ symmetry.

The high-energy data reveal a rearrangement effect in the intensity of the B_{1g} and $A_{1g}+B_{2g}$ symmetries similar to the

effect seen in Y-123 compounds.[6,30] The low-energy border of the effect is close to the region where the gap feature occurs. The rearrangement has its maximum around 1500 cm^{-1} and extends to a roughly 3000 cm^{-1} Raman shift. We interpret this in terms of an interaction between the remaining antiferromagnetic order and incoherent electronic states. The resonance enhancement of the rearrangement supports this assignment and is qualitatively in agreement with a prior investigation carried out in slightly underdoped Y-123 compounds.[6]

Our experimental results show that the rearrangement is likely to be a general property of the high-temperature superconductors. It reveals a subtle interplay between electronic and magnetic excitations. The decrease of scattering intensity in A_{1g} geometry can be related to observations from other techniques, namely, SIN and SIS tunneling spectroscopy and ARPES. This decrease of intensity in A_{1g} geometry occurs along with the enhancement of scattering intensity in B_{1g} geometry, revealing an enhanced coherence of the electronic and magnetic excitations below T_c. It seems likely that a description of the gap feature, without understanding the properties of the high-energy Raman continuum, is rather incomplete.

ACKNOWLEDGMENTS

M.R. thanks U. Merkt, A. Bock, G. Blumberg, R. Hackl, M. Norman, D. Manske, C. T. Rieck, S. Osterthun, and O. A. Hammerstein for many interactive discussions and their encouragement. We acknowledge financial support of the DFG via a grant of the Graduiertenkolleg ''Physik nanostrukturierter Festkörper'' and the NSF through the STCS via DMR 91-20000.

[1] J. R. Kirtley, C. C. Tsuei, M. Rupp, J. Z. Sun, Lock See Yu-Jahnes, A. Gupta, M. B. Ketchen, K. A. Moler, and M. Bhushan, Phys. Rev. Lett. **76**, 1336 (1996).

[2] Z.-X. Shen, D. S. Dessau, B. O. Wells, D. M. King, W. E. Spicer, A. J. Arko, D. Marshall, L. W. Lombardo, A. Kapitulnik, P. Dickinson, S. Doniach, J. DiCarlo, A. G. Loeser, and C. H. Park, Phys. Rev. Lett. **70**, 1553 (1993).

[3] T. P. Devereaux, D. Einzel, B. Stadlober, R. Hackl, D. H. Leach, and J. J. Neumeier, Phys. Rev. Lett. **72**, 396 (1994).

[4] Y. De Wilde, N. Miyakawa, P. Guptasarma, M. Ivaravrone, L. Ozyuzer, J. F. Zasadinski, P. Romano, D. G. Hinks, C. Kendziora, G. W. Crabtree, and K. E. Gray, Phys. Rev. Lett. **80**, 153 (1998).

[5] M. R. Norman, H. Ding, J. C. Campuzano, T. Takeuchi, M. Randeria, T. Yokoya, T. Takahashi, T. Mochiku, and K. Kadowaki, Phys. Rev. Lett. **79**, 3506 (1997).

[6] M. Rübhausen, C. T. Rieck, N. Dieckmann, K.-O. Subke, A. Bock, and U. Merkt, Phys. Rev. B **56**, 14 797 (1997).

[7] K. B. Lyons, P. A. Fleury, L. F. Schneemeyer, and J. V. Waszczak, Phys. Rev. Lett. **60**, 732 (1988).

[8] G. Blumberg, R. Liu, M. V. Klein, W. C. Lee, D. M. Ginsberg, C. Gu, B. W. Veal, and B. Dabrowski, Phys. Rev. B **49**, 13 295 (1994).

[9] D. Reznik, S. L. Cooper, M. V. Klein, W. C. Lee, D. M. Ginsberg, A. A. Maksimov, A. V. Puchkov, I. I. Tartakovskii, and S-W. Cheong, Phys. Rev. B **48**, 7624 (1993).

[10] B. Friedl, C. Thomsen, and M. Cardona, Phys. Rev. Lett. **65**, 915 (1990).

[11] M. Cardona, T. Strohm, and J. Kircher, Proc. SPIE **2696**, 182 (1996).

[12] R. Hackl, W. Glaser, P. Müller, D. Einzel, and K. Andres, Phys. Rev. B **38**, 7133 (1988).

[13] M. Rübhausen, N. Dieckmann, A. Bock, U. Merkt, W. Widder, and H. F. Braun, J. Low Temp. Phys. **105**, 761 (1996).

[14] N. Dieckmann, M. Rübhausen, A. Bock, M. Schilling, K.-O. Subke, U. Merkt, E. Holzinger-Schweiger, Physica C **272**, 269 (1996).

[15] P. Knoll, C. Thomsen, M. Cardona, and P. Murugaraj, Phys. Rev. B **42**, 4842 (1990).

[16] K. B. Lyons, P. A. Fleury, J. P. Remeika, A. S. Cooper, and T. J. Negran, Phys. Rev. B **37**, 2353 (1988).

[17] G. Blumberg, P. Abbamonte, M. V. Klein, W. C. Lee, D. M. Ginsberg, L. L. Miller, and A. Zibold, Phys. Rev. B **53**, 11 930 (1996).

[18] M. Rübhausen, N. Dieckmann, A. Bock, U. Merkt, W. Widder, and H. F. Braun, Phys. Rev. B **53**, 8619 (1996).

[19] M. Rübhausen, N. Dieckmann, A. Bock, and U. Merkt, Phys. Rev. B **54**, 14 967 (1996).

[20] M. Yoshida, N. Koshizuka, and S. Tanaka, Phys. Rev. B **42**, 8760 (1990).

[21] R. Liu, C. Thomsen, W. Kress, M. Cardona, B. Gegenheimer, F. W. de Wette, J. Prade, A. D. Kulkarni, and U. Schröder, Phys. Rev. B **37**, 7971 (1988).

[22] R. Liu, M. V. Klein, P. D. Han, and D. A. Payne, Phys. Rev. B **45**, 7392 (1992).

[23] A. A. Martin and M. J. G. Lee, Physica C **254**, 222 (1995).

[24] D. K. Morr and A. V. Chubukov, Phys. Rev. B **56**, 9134 (1997).

[25] B. S. Shastry and B. I. Shraiman, Int. J. Mod. Phys. B **5**, 365 (1991).

[26] G. Blumberg, Moonsoo Kang, M. V. Klein, K. Kadowaki, and C. Kendziora, Science **276**, 1427 (1997).

[27] M. V. Klein and S. B. Dierker, Phys. Rev. B **29**, 4976 (1984).

[28] D. Manske, C. T. Rieck, R. Das Sharma, A. Bock, and D. Fay, Phys. Rev. B **56**, 2940 (1997).

[29] M. Kang, G. Blumberg, M. V. Klein, and N. N. Kolesnikov, Phys. Rev. Lett. **77**, 4434 (1996); M. Kang, Ph.D. thesis, University of Urbana, 1997.

[30] M. Rübhausen, N. Dieckmann, K.-O. Subke, A. Bock, and U. Merkt, Physica C **280**, 77 (1997).

[31] M. Lax, J. Appl. Phys. **48**, 3919 (1977).

[32] A. V. Inyushkin, A. N. Taldenkov, L. N. Demganets, T. G. Uvarova, and A. B. Bykov, Physica B **194-196**, 479 (1994).

[33] C. Kendziora, R. J. Kelley, and M. Onellion, Phys. Rev. Lett. **77**, 727 (1996).

[34] D. Einzel and R. Hackl, J. Raman Spectrosc. **27**, 307 (1996).

[35] B. S. Shastry and B. I. Shraiman, Phys. Rev. Lett. **65**, 1068 (1990).

[36] A. Virosztek and J. Ruvalds, Phys. Rev. B **45**, 347 (1992).

[37] A. V. Chubukov and D. M. Frenkel, Phys. Rev. Lett. **74**, 3057 (1995).

[38] A. V. Chubukov and D. M. Frenkel, Phys. Rev. B **52**, 9760 (1995).

[39] Z. X. Shen and D. S. Dessau, Phys. Rep. **253**, 1 (1995).